

Detecting land use and land cover change for a 28-year period using multi-temporal Landsat satellite images in the Jukskei River catchment, Gauteng, South Africa.

Tshepo Mawasha¹ and Wilma Britz²

¹Department of Geoscience, Nelson Mandela University, Gqeberha, South Africa
s212355686@mandela.ac.za

²Department of Geoscience, Nelson Mandela University, Gqeberha, South Africa
wilma.britz@mandela.ac.za

DOI: <http://dx.doi.org/10.4314/sajg.v11i1.2>

Abstract

The Jukskei River catchment is one of the urban catchments in the central part of Gauteng province covering a large part of City of Johannesburg Metropolitan Municipality and small part of Tshwane and Ekurhuleni Metropolitan Municipalities that have witnessed tremendous land use/land cover (LULC) change over time. Jukskei River catchment is one of the fastest growing catchments in terms of population and change in LULC over time. Therefore, it is very important to detect the nature and extent of these changes in order to identify the direction and future expansion of LULC within the catchment area. To accomplish that, multi-temporal satellite remotely sensed data acquired from Landsat-5 Thematic Mapper (TM) 1987, Landsat-5 Thematic Mapper (TM) 2001 and Landsat-8 Operational Land imager (OLI) 2015 were used to detect LULC change in Jukskei River catchment area. The Jukskei River catchment was classified into four major LULC classes including: Built-up area, bare surface, sparse vegetation and intact vegetation. The analysis of the results revealed that for the past 28 years (i.e., 1987-2015), built-up and bare surface areas have increased by 56.2% (42713.1 ha) and 8.2% (6225.1 ha) while intact and sparse vegetation have decreased by 9.8% (7455.0 ha) and 25.8% (19659.6 ha), respectively. The overall accuracies for 1987, 2001, and 2015, were 85.9%, 87.5%, and 92.5% respectively, with Kappa Index of Agreement (KIA) of 81.3%, 83.3%, and 90% which indicates the accuracy of classified images with the reference images. The results revealed by this study can be used for decision-making activities and policy development regarding land use management within the catchment.

Keywords: *Jukskei River catchment, remote sensing, Landsat Images, land use/land cover, Change Detection.*

1. Introduction

Land use/land cover (LULC) change is one of the most important processes related to global change (Foley *et al.*, 2005). LULC has been acknowledged as chief drivers of environmental change at all spatial and temporal levels (Mishra *et al.*, 2014). Humans play a major role as forces of change in the environment, influencing changes at all levels ranging from local to global (Paiboonvorachat and Oyana, 2011). Among others, there are many driving forces contributing to LULC change which could be social, economic, institutional, political or geographic in nature (Lepers *et al.*, 2005). These direct drivers impact at several levels such as local conditions (subsistence livelihood, poverty and culture); at national levels (population growth, domestic markets, state policies, legislations and laws) and at the international level (world markets' demands, commodity prices for goods and services) (Koranteng *et al.*, 2016). Therefore, reliable and updated information on the LULC maps and their dynamics can help to provide base information for further decision-making in catchment management activities (Alphan, 2003).

Long-term image archives of the earth resource satellites are a useful resource for LULC change detection studies. Yuan *et al.*, (2005) developed a methodology to map and monitor LULC change using multi-temporal Landsat TM data in the seven-county Twin Cities Metropolitan Area of Minnesota for 1986, 1991, 1998 and 2002. Their result showed that between 1986 and 2002 the amount of urban land increased from 23.7% to 32.8% of the total area, while rural cover types of agriculture, forest and wetland decreased from 69.6% to 60.5%. Amin *et al.*, (2012) carried out a study on LULC cover mapping of Srinagar city in Kashmir Valley. They observed that the Srinagar city has experienced significant changes during 1990 to 2007. The analysis also showed that changes in land use pattern have resulted in the loss of forest area, open spaces, etc. Rawat *et al.*, (2013) have carried out a study on LULC of five major towns (i.e., Ramnagar, Nainital, Bhimtal, Almora and Haldwani) of Kumaun Himalaya in Uttarakhand (India). Based on 20 years of satellite data from 1990 to 2010, they found that the built-up area has been increased about 8.9% and 3.9%, respectively, while area under other land categories such as vegetation, agricultural land and water body have decreased about 9.4%, 0.7% and 2.8%, respectively.

The Jukskei River catchment has experienced rapid industrial development, increase in built-up areas and population growth. Detecting the past and the present LULC conditions play a key role in decision-making when managing human activities within the catchment area. However, within the Jukskei River catchment, there is limited number of research studies that has been made in analysing and detecting LULC change using GIS and RS to capture the patterns, trends and drivers of landscape changes over time. However, multi-temporal remote sensing data contained much more information which benefit for improving LULC classification accuracy, mainly because different vegetation types usually had different growth characteristics and presented different spectral features in different periods (Shao *et al.*, 2001; Jia *et al.*, 2013; Odindi *et al.*, 2012; Li *et al.*, 2014). Therefore, this paper is based on application of multi-temporal remotely sensed data using a GIS and RS techniques approach in mapping, detecting, analysing the annual LULC change rate for the past 28 years from 1987 to 2015. The results achieved through this study provide support for decision-making and

understanding of drivers that contribute to LULC change within the catchment, which are required to assist with LULC practices for sustainable development.

2. Materials and research methods

2.1. Description of the Study Area

The Jukskei River catchment is one of the largest catchment areas in Gauteng Province with the City of Johannesburg Metropolitan Municipality covering a large portion of the catchment area followed by Tshwane Municipality and Ekurhuleni Metropolitan Municipality. The catchment is located at South Latitude 26° 08' and East Longitude 28° 14'. The elevation of the downstream catchment ranges from 1319.12 m to 1497.62 m and the upstream catchment is characterised by an elevation ranging between 1378.08 m and 1802 m. The catchment area covers an area of approximately 800 km² with the Jukskei River being the longest river among others (Figure 1). The catchment is characterized by a relatively dry and sunny climate. Temperatures are usually fairly mild due to the city's altitude, with an average maximum daytime temperature of 25 °C in the summer, dropping to around 17 °C in winter. The study area has different land uses, including industrial, trade, educational facilities, tourism destinations, places of entertainment all dominated by vast areas of predominantly built-up areas. The Jukskei River is the largest river within the catchment area with a total length of about 68 km and is joined by numerous tributaries. Additionally, the catchment is gauged and has five gauging stations with scattered and one located at the catchment outlet: there is also one global weather station (i.e., Climate Forecast System Reanalysis) and two South African weather stations.

2.2. Satellite Data Acquisition

Landsat data provide the longest terrestrial remote sensing record and have a long history for land cover mapping because of their moderate spatial resolution and near global coverage (Roy *et al.*, 2014; Wulder *et al.*, 2016). With the freely available Landsat data, it is now possible to reconstruct the history of the Earth's surface back to 1972 (Pflugmacher *et al.*, 2012). In this study, three cloud-free summer images acquired by Landsat satellites in 1987, 2001 and 2015 (Table 1) were downloaded from the U.S Geological Survey (USGS) Centre for Earth Resources Observation and Science (EROS) (<https://earthexplorer.usgs.gov/>).

Table 1: Satellite image acquisition dates and specifications.

Satellite Sensor	Path/Row	Date of acquisition	Resolution (meters)	Spectral bands
Landsat-5 TM	170/078	06-Jan-87	30	7
Landsat-5 TM	170/078	13-Feb-01	30	7
Landsat-8 OLI	170/078	20-Feb-15	30	11

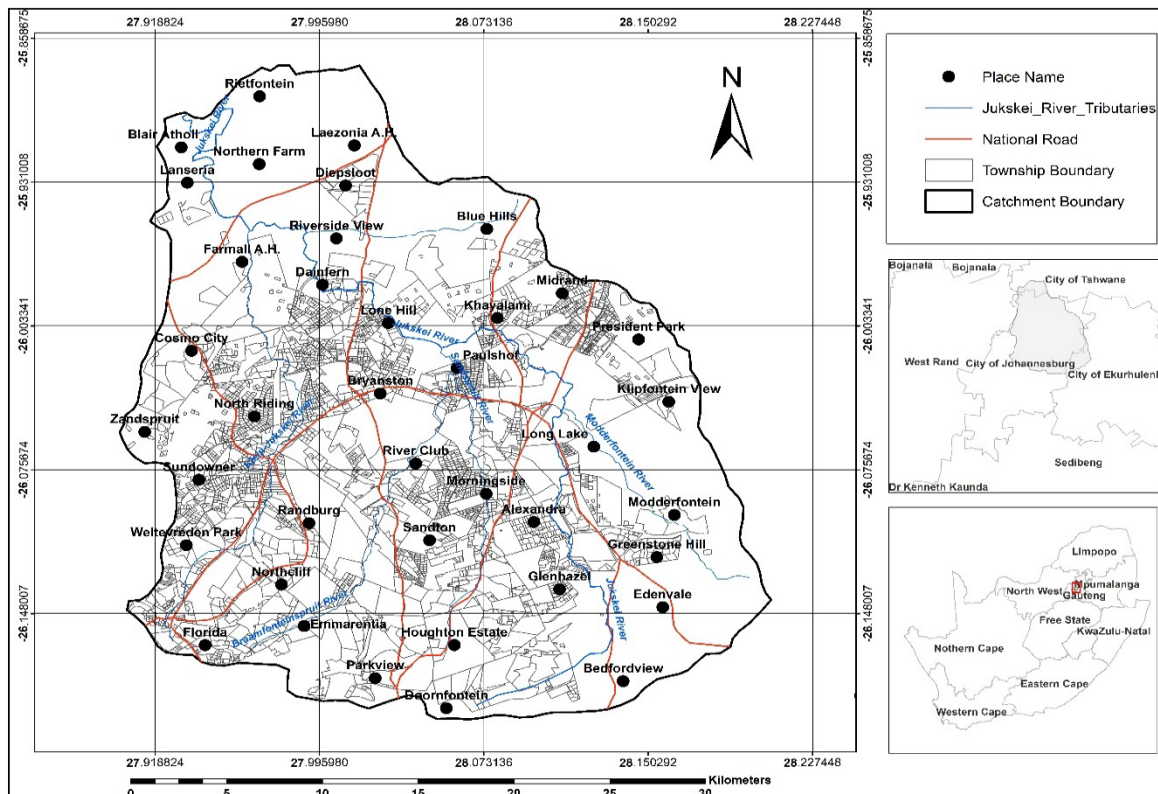


Figure 1: Location of the study area

2.3. Atmospheric Correction of Landsat Images

Topographic correction is the process of reducing variation of image values resulting from differences in surface terrain illumination and shadows cast during image acquisition (Vanonckelen *et al.*, 2013). Atmospheric correction aims at determining the true surface reflectance values by removing the atmospheric effects resulting from the scattering and absorption of electromagnetic radiation by gases and aerosols when passing through the atmosphere to the satellite sensor (Hadjimitsis *et al.*, 2010). Many studies have acknowledged that atmospheric correction is one of the most important corrections in land cover classification, especially when working with multiple and multi-temporal scenes (Song *et al.*, 2001; Young *et al.*, 2017).

For the purpose of this study the atmospheric correction algorithm was performed using Dark Object Subtraction to remove the atmospheric effects resulting from the scattering and absorption of

electromagnetic radiation by gases and aerosols when passing through the atmosphere to the satellite sensor (Hadjimitsis *et al.*, 2010). The Dark Object Subtraction approach argues that there can be a substantial likelihood that at least a few pixels in an image should be black. (i.e., 0% Reflectance) (Chavez, 1988). Therefore, Semi-Automatic Classification plugin in Quantum Geographical Information System (QGIS) was used for pre-processing of Landsat images (i.e., Landsat-5 TM, and Landsat-8 OLI) by applying DOS atmospheric correction. Equation 1 illustrates the DOS atmospheric correction method where the lowest image digital values (DN) are subtracted from all other DN values across an image:

$$L_{\lambda} = L_{s\lambda} + L_p \quad [1]$$

where:

L_{λ} is the corrected DN value, $L_{s\lambda}$ is the original DN value and L_p is the DN value of the dark pixels (Chavez, 1988; Song *et al.*, 2001).

2.4. Image Classification and Change Detection Techniques

In this study image classification was performed by capturing different pixels and assigning them to certain classes in accordance with the information categories provided by the users (Perumal & Bhaskaran, 2010). Anderson *et al.*, (1976) point out that there is no ideal classification for LULC, the process is subjective, depending on the different perspectives in the classification process. For this study, a supervised maximum likelihood classification method was applied. The maximum likelihood method is a common method in remote sensing owing to its robustness and was therefore implemented to classify the images (Strahler, 1980; Ediriwickrema & Khorram, 1997; Zheng *et al.*, 2005; Mawasha & Britz, 2020).

Prior to image classification, training areas were captured using a false colour composite for each of the satellite images of 1987, 2001 and 2015 by selecting a minimum of 10 pixels per polygon. In this study, four classes of LULC (i.e., built-up area, degraded vegetation, bare surface, and intact vegetation) were selected with the use to google earth image (see Table 2). To determine the changes in LULC in different years, a post-classification change detection algorithm was used in this study. Post classification comparison is a common method used for change detection (Alphan *et al.*, 2009; Mas, 1999; Chen *et al.*, 2003). This method detects changes in land cover type by comparing pixel by pixel for the classified images. The use of the post classification comparison technique resulted in a cross-tabulation matrix (i.e., LULC change transition matrix) which was computed using the CROSSTAB module in the TerrSet Geospatial Monitoring and Modelling software. A transition matrix is a fundamental starting point for the analysis of land change (Pontius *et al.*, 2004). Gross gains and losses were calculated for one period covering 28 years (i.e., 1987-2015) to detect changes and LULC transformation among LULC classes and to identify.

Table 2: Description of LULC classes in the Jukskei River catchment area.

LULC type	Description
1. Built-up area	This group applies to regions of high population growth, suburban, commercial and business areas, roads / flooring and leisure facilities.
2. Bare surface	This group covers regions not protected by trees, fields with exposed soils, degraded soils and mined areas.
3. Intact vegetation	This category applies to areas covered by dense vegetation, cropland, agricultural land and natural landscaping.
4. Sparse vegetation	It consists of areas of scattered vegetation, areas of shrubs covering and small wooded trees mixed with grasses. This group applies to areas with very little vegetation coverage.

Table 3: LULC change transition matrix for comparing two maps between observation times (Source: Munthali, Botai, Davis, & Abiodun, 2019).

		Time 2 (T2)					Total T1	Loss
		LULC1	LULC2	LULC3	LULC4	LULC5		
Time 1 (T1)	LULC1	A_{11}	A_{12}	A_{13}	A_{14}	A_{15}	A_{1+}	$A_{1+} - A_{11}$
	LULC2	A_{21}	A_{22}	A_{23}	A_{24}	A_{25}	A_{1+}	$A_{2+} - A_{22}$
	LULC3	A_{31}	A_{32}	A_{33}	A_{34}	A_{35}	A_{1+}	$A_{3+} - A_{33}$
	LULC4	A_{41}	A_{42}	A_{43}	A_{44}	A_{45}	A_{1+}	$A_{4+} - A_{44}$
	LULC5	A_{51}	A_{52}	A_{53}	A_{54}	A_{55}	A_{1+}	$A_{5+} - A_{55}$
	Total T2	A_{+1}	A_{+2}	A_{+3}	A_{+4}	A_{+5}	1	
Gain		$A_{+1} - A_{11}$	$A_{+2} - A_{22}$	$A_{+3} - A_{33}$	$A_{+4} - A_{44}$	$A_{+5} - A_{55}$		

As shown in Table 3, the computed LULC change transition matrix consisted of rows (displaying LULC class category for time 1, T1) and columns (displaying LULC class category for time 2, T2). The notation A_{12} denotes the proportion of the landscapes which experiences a transition from LULC1 to LULC2. The diagonal entries indicate the total amount of persistence, which dominates most landscapes, including those where authors claim that the change is important and/or large (Wear & Bolstad, 1998; Mertens and Lambin, 2000; Geoghegan *et al.*, 2001; Chen *et al.*, 2002). In the Total column (i.e., total T1), the notation A_{1+} denotes the proportion of the landscape in LULC1 in time 1, which is the sum over all 1. In the Total row, the notation A_{+1} denotes the proportion of the landscape in LULC1 in time 2, which is the sum over all 1. The additional column on the right indicates the proportion of the landscape that experiences gross loss of LULC1 between time 1 and time 2. The bottom row indicates the proportion of the landscape that experiences gross gain of LULC1 between time 1 and time 2.

2.5. Annual LULC change rate for the period of 1987–2001, 2001–2015, and 1987–2015

After classifying all the images, the trend and rate of LULC changes in the catchment area was determined by subtracting the total area for each identified classes of 1987 from 2001, 2001 from 2015 and 1987 from 2015 which the outcomes could be positive (increasing) or negative (decreasing). The percentage and rate of LULC change were computed by the following formula (Kindu *et al.*, 2013; Demissie *et al.*, 2017):

$$\text{Percentage of change} = \frac{A - B}{B} \times 100 \quad [2]$$

$$\text{Rate of change (ha/year)} = \frac{A - B}{T} \quad [3]$$

where:

A and B are the final and initial area coverage of LULC types during that specific period, and *T* represents year difference between the initial and final period. A LULC classified image for 1987 was used as the initial image and the 2015 image as the final image and a change statistics table was created for analysis.

2.6. Accuracy Assessment

In remote sensing, accuracy assessment is mandatory and is important for providing information about the quality of the produced classification (Okeke & Karnieli, 2006; Rwanga & Ndambuki, 2017). For the purpose of this study, a confusion error matrix was used for the assessment. The confusion matrix shows errors resulting from missing and mixing of information, various accuracy measurements, such as the overall accuracy, producer's accuracy, user's accuracy and Kappa Index Agreement (KIA) (Zhou & Xiong, 2012). In order to assess the accuracy of the classification method, a stratified random sampling method was applied to select 50 points per class i.e., 200 points for each classified image. With the aid of the aerial photo mosaic (1:25 000), invariant feature points and topographic sheets, the accuracy of the images was assessed using the error matrix technique described by Congalton & Plourde (2002). The user's accuracy, producer's accuracy, overall accuracy as well as Kappa coefficient were calculated as follows:

User accuracy is the likelihood that a pixel relates to a certain group of LULCs as defined by Petropoulos, Kalaitzidis & Vadrevu (2012); the algorithm properly identifies the pixels within the same class. It displays the percentage of likelihood the that class on the ground is actually defined by the class in which a pixel is identified into an image (Story & Congalton, 1986). The sum of the row is calculated by dividing each diagonal part into one confusing matrix:

$$\text{User Accuracy} = \frac{\text{Total number of correctly correct pixels in a category}}{\text{Total reference pixels (i.e., column total)}} \times 100 \quad [4]$$

Although the accuracy of the producer is an indicator of the accuracy of a specific classification system, it indicates the correctly categorized percentage of a particular ground class. The diagonal elements in the table are divided by the sum of each column by dividing:

$$\text{Producer Accuracy} = \frac{\text{Total number of correct pixels in a category}}{\text{Total reference pixels (i.e., row total)}} \times 100 \quad [5]$$

Overall accuracy is the number of pixels that have been accurately identified from the validity data collection over the overall number of pixels used as a percentage for the accurate measurement (Petropoulos, Kalaitzidis & Vadrevu, 2012).

$$\text{Overall Accuracy} = \frac{\text{Total number of pixels accurately classified}}{\text{Total number of referenced pixels}} \times 100 \quad [6]$$

The Kappa Index of Agreement (KIA) is the most widely used metric to determine the degree of agreement between the comparison and validation datasets, as stated by Foody (2010). It indicates the degree of reliability of image classification. The KIA statistical range is between zero and one. The KIA is determined according to Congalton (1991) formula:

$$\text{KIA} = \frac{N \sum_{i=1}^k x_{ii} - \sum_{i=1}^k (x_{i+} \times x_{+i})}{N^2 - \sum_{i=1}^k (x_{i+} \times x_{+i})} \quad [7]$$

where:

N = Total sum of correct pixels, x_{ii} = Diagonal cells of the error matrix, x_{i+} = Total of observation in row i (right of matrix), x_{+i} = Total of observations in column i (bottom of the matrix). Kappa values have also been categorized into three possible ranges; value greater than 0.80 (i.e., > 80%) signifies strong agreement; between 0.40 and 0.80 (i.e., 40 – 80%) signifies moderate agreement; below 0.40 (i.e., < 40%) signifies poor agreement (Congalton and Green, 2009), and this ranges were employed in this study to assess the accuracy.

3. Results and discussion

3.1. Spatio-temporal distribution of LULC Change from 1987 to 2015

Figure 2 (a-c) shows the LULC classification maps for 1987, 2001 and 2015 that were generated by using the maximum likelihood method. Four distinguishable LULC classes were identified in this study, these are built-up area (BA), bare surface (BS), intact vegetation (IV) and sparse vegetation (SV). From the classified images, the results indicated that there were noticeable changes in the built-up areas, intact vegetation and sparse vegetation LULC classes within the Jukskei River catchment area over the last 28 year period. Large portions of sparse and dense vegetation declined and were converted into built-up areas.

Between 1987 and 2015, the built-up area increased from 28700.4 ha (37.7%) in 1987 to 36313.6 ha, 47.8% of the total catchment area in 2001; and increased to 56.2%, covering an area of 42713.1ha in 2015 indicating 18.5% of an areal increment of the total catchment area (Table 4). The total area

of the catchment area covered by bare surface was 3482.9 ha (4.8%) in 1987, however, in 2001 the coverage increased to 6550.3ha (8.6%). This declined again to 6225.1ha (8.2%) in 2015. A change in the total area of sparse vegetation was also observed. Classification indicated that the sparse vegetation covered 27715.4 ha in 1987 constituting about 36.4% of the total area of the catchment area and this area was reduce to 14621.4 ha in 2001 covering 19.2% and increased again in 2015 by 25.8% covering an area of 19659.6 ha of the catchment area. Thus, approximately 10.6% of the sparse vegetation diminished in 28 years. This might be due to an increase in anthropogenic activities that led to gradual conversion of other LULC classes into built-up areas or human development areas as the area faced significant increase in population during the past decades within the catchment area.

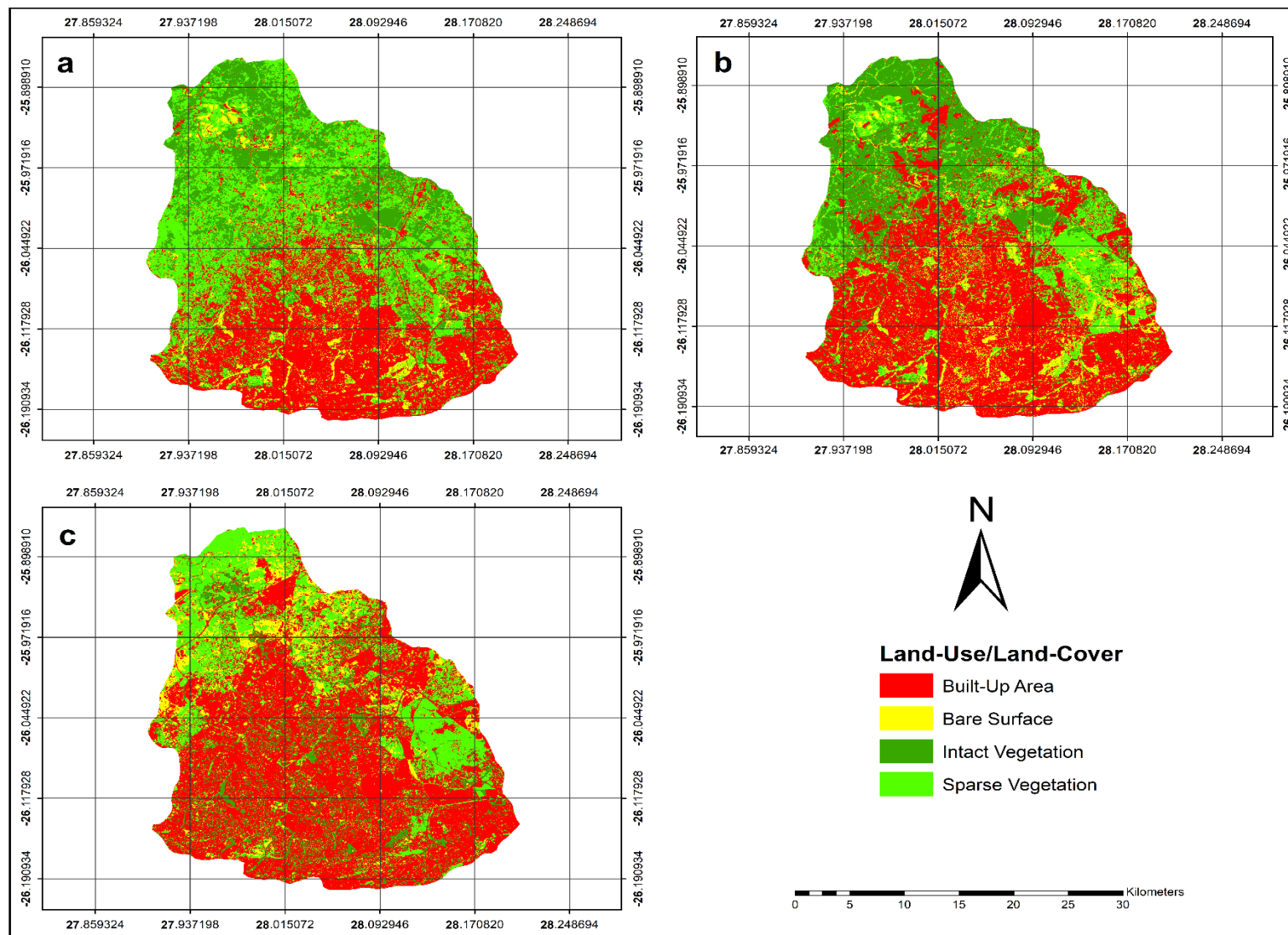


Figure 2: LULC change maps over time for the study area (a) 1987; (b) 2001; and (c) 2015.

Table 4: LULC change of the Jukskei River catchment area during 1987–2015

LULC Classes	LULC area (ha) and %						Change in LULC (ha) and %					
	1987		2001		2015		1987-2001		2001-2015		1987-2015	
	Area (ha)	%	Area (ha)	%	Area (ha)	%	Area (ha)	%	Area (ha)	%	Area (ha)	%
BA	28700.4	37.7	36313.6	47.8	42713.1	56.2	+6399.5	17.6	+7613.2	26.5	+14012.7	48.8
BS	3482.9	4.6	6550.6	8.6	6225.1	8.2	+3067.7	88.1	-325.5	-5	+2742.2	78.7
IV	16154.1	21.2	18567.3	24.4	7455.0	9.8	+2413.2	14.9	-11112.3	-60	-8699.1	-53.9
SV	27715.4	36.4	14621.4	19.2	19659.6	25.8	-13094	-47.2	+5038.2	34.51	-8055.8	-29.1
Total	76052.8	100	76052.8	100	76052.8	100	-	-	-	-	-	-

- Indicates loss in LULC class

+ Indicates gain in LULC class

3.2. Accuracy assessment of the classified images

The classification accuracy for the LULC maps derived from satellite data was assessed using three different time periods by means of a confusion error matrix. Assessment of the classification results proved that the supervised maximum likelihood classification produced valid and reliable LULC maps since all the overall accuracies and the KIA were higher than 80% (Congalton and Green, 2009). The overall accuracies for 1987, 2001, and 2015, were 85.9%, 87.5%, and 92.5% respectively, with KIA of 81.3%, 83.3%, and 90% which indicates the accuracy of classified images with the reference images. Producer's and user's accuracies were also high, ranging from 70% to 100%. The Landsat-5 TM data resulted in the lowest overall accuracy (85.9%) and KIA (81.3%) of the three datasets. The low spatial resolution combined with the spectral similarity of built-up and bare surface areas made it difficult to separate these two classes on the Landsat-5 TM imagery. Furthermore, a decrease of image spatial resolution leads to spectral mixing of different categories which produce spectral confusion between cover materials (Yang and Lo, 2002). As stated by Anderson *et al.*, (1976) a reliable land cover classification needs the minimum overall accuracy value computed from an error matrix to be 85%. Therefore, the overall accuracies for the study periods are in agreement with findings of other studies. Hence, the results revealed by this study can be used by land use policy makers and catchment managers for decision-making activities and policy development regarding land use management within the catchment.

3.3. Spatio-temporal changes over time (1987-2001, 2001-2015 and 1987-2015)

In this study, LULC change detection of each LULC for the last three decades was examined between years (i.e., 1987-2001, 2001-2015 and 1987-2015) and the relative changes were obtained in both hectares and percentage see Table 4 and Figure 3. The analysis of the results reveals that there was increase in areal coverage of built-up areas during 1987–2001 (Table 4) – from 6399.5 ha (26.5%) to 7613.2 ha (17.6%) during 2001 to 2015. The analysis of LULC change for the last 28-years (between 1987 and 2015) shows a remarkable areal increment of 14012.7ha (48.8%) for built-up area class. This increase in built-up area may possibly be the result of the growing demand for new housing and settlements, as well as other administrative developments within and surrounding the study area (see Figure 2 & 4). There was an increase of bare surfaces by 3067.7ha in the first period between 1987 and 2001 that is a gain of 88.1%.

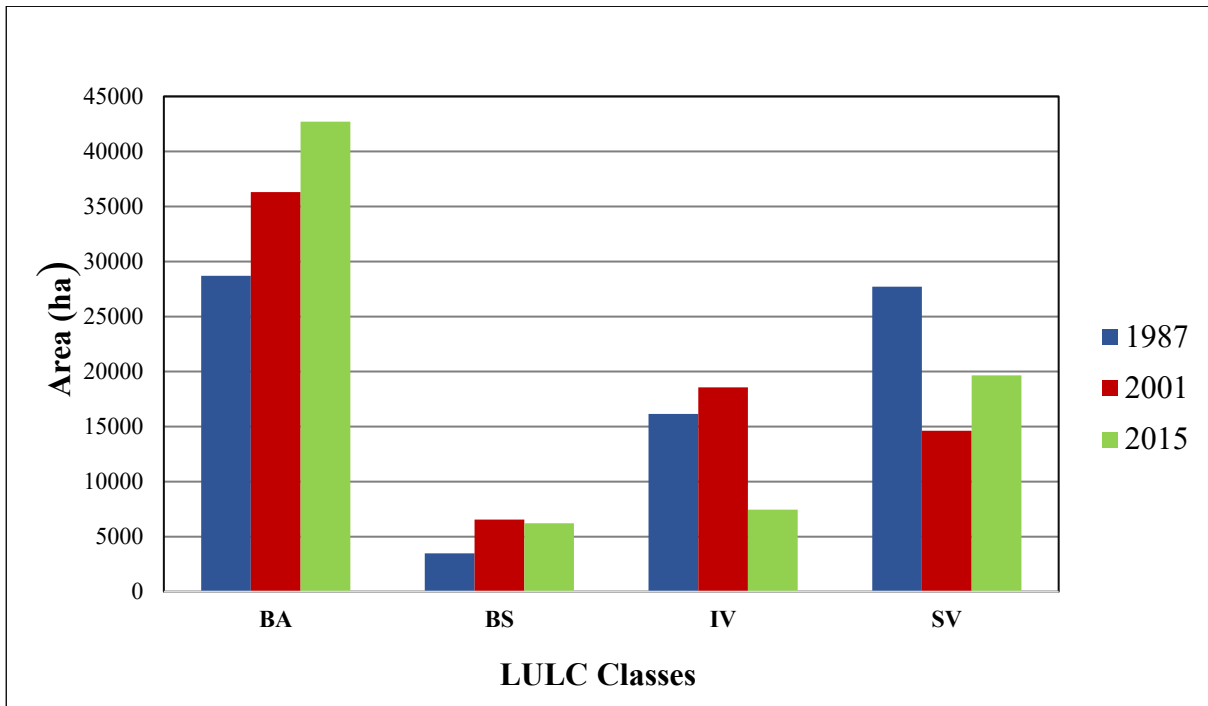


Figure 3: LULC change from 1987 to 2015.

However, in the second period between 2001 and 2015 the share of bare surface coverage decreased slightly by 325.5 ha (5% lost). Therefore, over the 28-year period, that is from 1987 to 2015, the share has increased by 78.7% (2742.2 ha). Intact vegetation was increased by 2413.2 ha (14.9%) during the first period from 1987 to 2001. However, an intensive decline was observed during the second period from 2001 to 2015 by 11112.3 ha (60% lost). Furthermore, in the last 28 years, about 53.9% (8699.1ha) of intact vegetation land was lost and changed into other LULC classes. The sparse vegetation during the first period 1987 and 2001 decreased by 13094 ha (47.2% lost). However, in the second period between 2001 and 2015 the share of sparse vegetation coverage has increased by 34.5% due to shrinkage of intact vegetation and bare surface during the same periods. These radical changes in natural land cover are mostly attributable to human activities and urbanization and may have resulted in an increase in demand for arable land for administrative or settlement development, as is common practice in the study area (see Figure 2 & 3).

3.4. Annual LULC Change rate for the period 1987-2015

Table 5 represents annual LULC change rate for built-up areas, bare surface, intact vegetation and sparse vegetation between studied periods of 1987-2001 (first period), 2001-2015 (second period) and 1987-2015 (whole period). In terms of annual change rate, the built-up area shows a very high positive increase compared to other LULC types during the study period (Table 5). The analysis indicated that during the second study period 2001 and 2015, built-up area and sparse vegetation has increased at a rate of 543.8 ha/year (26.5% gain), 359.9 ha/year (34.1% gain), in the same period bare surface and intact vegetation decreased by 23.25 ha/year (5% loss) and 793.7 ha/year (60% loss) respectively. Likewise, during first study period 1987 and 2001 an expansion of built-up area with an

increase rate of 457.8 ha/year (17.6 % gain) was noticed. This might be due to residential development within the catchment area because during the same period, sparse vegetation rapidly decreased by 935.3 ha/year (47.2% loss).

Table 5: Annual LULC change rate in hectares as a percentage

LULC Classes	Annual LULC change rate (ha/year)					
	1987-2001		2001-2015		1987-2015	
	Area (ha)	%	Area (ha)	%	Area (ha)	%
Built-up area	457.1	17.6	543.8	26.5	500.5	48.8
Bare surface	219.1	88.1	-23.25	- 5	97.9	78.7
Intact vegetation	172.4	14.9	- 793.7	- 60	-310	- 53.9
Sparsed vegetation	- 935.3	- 47.2	359.9	34.5	- 287.7	- 29.1

– Indicates loss in LULC class

Over the last 28 year (i.e., 1987-2015) period, expansion of built-up areas and bare surface increased at a rate of 500.5 ha/year (48.8% gain) and 97.9 ha/year (78.7% gain) respectively, contrary to this the intact vegetation and sparse vegetation shrunk with a rate of 310 ha/year (53.9% lost) and 287.7 ha/year (29.1% lost), respectively (Table 5). The annual LULC change rate for built-up area during 1987-2001 period is higher with 543.8 ha/year (26.5%) compared to period during 1987-2015 with 500.5 ha/year (48.8%). This might be attributed by differences of years (i.e., 28 years) between the initial (i.e., 2015) and final period (i.e., 1987) compared to 1987-2001 and 2001-2015 which yield difference of 14 years. Within the Jukskei River, built-up area compared to other LULC classes shows a positive growth which will have an effect on catchment hydrological response and other associated environmental problems.



3.5. LULC Transformation for the past 28-years (1987-2015)

The classified images of 1987 and 2015 were further analysed using a cross-tabulation (CROSSTAB) module of TerrSet software to detect LULC transformation that occurred within the Jukskei River catchment area. Table 6 shows the result of LULC transformations which denotes the amount of area in LULC features transformed from pre-existing state to another in the study area during 1987–2015. The matrix is comprised of the early year (1987) in the column axis with similar classes from the later year (2015) on the row axis. The matrix provides probabilities that reflect the statistics of the direction of LULC change. The higher transformations were experienced in sparse vegetation and intact vegetation. During the study period, out of 10574 ha that was built-up area in

1987, 7737 ha was still built-up area in 2015 but 1390 ha was converted to sparse vegetation, and the rest to bare surface and intact vegetation by 153 ha and 1294 ha respectively. At the same time the increase of built-up area, from 1987 to 2015, was mainly from sparse vegetation (5218 ha). The analysis of the study further revealed that intact vegetation decreased from 6016 ha in 1987 to 2684 ha in 2015. It retained 159 ha of it and was mainly replaced by built-up area and sparse vegetation. The class which replaced intact vegetation in 2015 was built-up area with an aerial coverage of 1294 ha. Bare surface class retained 13183 ha, almost 75% of the total 14369 ha in 1987. It was reduced to 1037 ha and mainly replaced by sparse vegetation, intact vegetation and built-up area in 2015 (Table 6). The analysis of the classified images over time revealed that, built-up areas are generally expected to increase in aerial coverage compared to other LULC classes due to residential development or demand within the Jukskei River catchment.

Table 6: LULC Transformation matrix for the past 28-years (1987-2015)

LULC classes		Initial stage 1987 Area (hectares)				Total
		BA	BS	IV	SV	
Final stage 2015	BA	7737	524	2494	5218	15973
	BS	153	13183	962	1037	15335
	IV	1294	461	159	770	2684
	SV	1390	201	2401	3225	7217
	Total	10574	14369	6016	10250	41209
Class difference		+ 5399	+ 966	-3332	-3033	0

 No change
 Change

4. Conclusion

This study demonstrated the efficiency of remote sensing Landsat data and GIS tools to develop a model that was used to detect LULC changes for a period of 28 years (i.e., 1987-2015). The analysis of the study revealed that there has been a change in LULC classes within the catchment area. Compared to other LULC classes such as bare surface, sparse vegetation and dense vegetation, the built-up area class increased in spatial extent throughout the period. This was due to industrial and residential development that is continuously increasing due to increase in population density and industrial development where impervious surfaces are replaced by pervious surfaces. The trend however, shows that sparse vegetation and intact vegetation has no potential to recover to its original state, as revealed by high conversion of sparse and intact vegetation to built-up area for the last 28-years. Additionally, the analysis of the results revealed that more than half of the total catchment area is covered by built-up area in 2015 compared to 37.7% in 1987. This increases environmental risk

such as flash floods due to high surface runoff due to LULC change. The multi-temporal classified images provides details of the spatial distribution of LULC change that can be used for decision-making for developing policies for land use practices within the catchment area.

5. References

- Alphan, H., Doygun, H. & Unlukaplan, Y.I., (2009). Post-classification comparisons of land cover using multi-temporal Landsat and ASTER imagery: the case of Kahramanmaraş, Turkey. *Environmental Monitoring and Assessment*, 151, 327–336.
- Alphan, H. (2003). Land use change and urbanization in Adana, Turkey. *Land Degradation Development*, 14, pp. 483–494.
- Amin, A., Amin, A. & Singh, S.K. 2012. Study of Urban Land use Dynamics in Srinagar city using Geospatial Approach. *Bulletin of Environmental and Scientific Research*, 2, 18–24.
- Anderson, J.R., Hardy, E.E., Roach, J.T. & Witmer, R.E., 1976. A Land use and land cover classification system for use with Remote Sensor data: U.S. Geological Survey, 671, 1–34.
- Chavez, P.S. (1988). “An improved dark-object subtraction technique for atmospheric scattering correction of multispectral data”. *Remote Sensing of Environment*, 24, 459–479.
- Chen, J., Gong, P., He, C., Luo, W., Tamura, M. & Shi, P. (2002). Assessment of the urban development plan of Beijing by using a CA-based urban growth model. *Photogrammetric Engineering and Remote Sensing*, 68(10), 1063–1071.
- Chen, Z.J., Chen, J., Shi, P.J. & Tamura, M., (2003). An IHS-based change detection approach for assessment of urban expansion impact on arable land loss in China. *International Journal of Remote Sensing*, 24, 1353–1360.
- Congalton, R.G. (1991). A review of assessing the accuracy of classifications of remotely sensed data. *Remote Sensing of Environment*, 37, 35–46.
- Congalton, R.G., & Green, K. (2009). *Assessing the Accuracy of Remotely Sensed Data: Principles and Practices*. 2nd Edition, Lewis Publishers, Boca Raton.
- Congalton, R.G., & Plourde, L. (2002). Quality assurance and accuracy assessment of information derived from remotely sensed data. In: Bossler J, editor. *Manual of geospatial science and technology*. London: Taylor and Francis, 349–361.
- Demissie, F., Yeshitil, K., Kindu, M., & Schneider, T. (2017) Land use/cover changes and their causes in Libokemkem District of South Gonder, Ethiopia. *Remote Sens Appl Soc Environ* 8, 224–230.
- Ediriwickrema, J. & Khorram, S. (1997). Hierarchical maximum-likelihood classification for improved accuracy. *IEEE Transactions on Geoscience and Remote Sensing*, 35, 810–816.
- Foley, J.A., DeFries, R., Asner, G.P., Barford, C., Bonan, G., Carpenter, S.R., Chapin, F.S., Coe, M.T., Daily, G.C., Gibbs, H. K., Helkowski, J.H., Holloway, T., Howard, E.A., Kucharik, C.J., Monfreda, C., Patz, J.A., Prentice, C.I., Ramankutty, N. & Snyder, P.K. (2005). Global Consequences of Land Use. *Science*, 22, 570–574.
- Foody, G.M. (2010). Assessing the accuracy of land cover change with imperfect ground reference data. *Remote Sensing of the Environment*, 114, 2271–2285.
- Geoghegan, J., Villar, S.C., Klepeis, P., Mendoza, P.M., Ogneva-Himmelberger, Y., Roy Chowdhury, R., Turner, B.L. & Vance, C., 2001. Modeling tropical deforestation in the southern Yucatan peninsular region: comparing survey and satellite data. *Agriculture, Ecosystems and Environment*, 85(1–3), 25–46.
- Hadjimitsis, D.G., Papadavid, G., Agapiou, A., Themistocleous, K., Hadjimitsis, M., Retalis, A., Michaelides, S., Chrysoulakis, N., Toullos, L. & Clayton C.R.I., 2010. Atmospheric correction for satellite remotely sensed data intended for agricultural applications: impact on vegetation indices. *Natural Hazards and Earth System Sciences*, 10(1), 89–95.

- Jia, K., Wu, B.F. & Li, Q.Z. 2013. Crop classification using HJ satellite multispectral data in the North China Plain. *Journal of Applied Remote Sensing*, 7, 1–11.
- Kindu, M., Schneider, T., Teketay, D., & Knoke, T. (2013). Land use/cover change analysis using object-based classification approach in Munessa-Shashemene landscape of the Ethiopian highlands. *Remote Sensing*, 5, 2411–2435.
- Koranteng, A., Zawila-Niedzwiecki, T. & Adu-Poku, I. (2016). Remote Sensing Study of Land Use/Cover Change in West Africa. *Journal of Environment Protection and Sustainable Development*, 2(3), 17–31.
- Lepers, E., Lambin, E.F., Janetos, A.C., Defries, R., Achard, F., Ramankutty, N., & Scholes, R.J. (2005). A synthesis of information on rapid land-cover change for the period 1981–2000. *Bioscience*, 55(2), 115–124.
- Li, Q., Cao, X., Jia, K., Zhang M. & Dong. Q., 2014. Crop type identification by integration of high spatial resolution multispectral data with features extracted from coarse-resolution time-series vegetation index data. *International Journal of Remote Sensing*, 35, 6076–6088.
- Mas, J.F. (1999). Monitoring land-cover changes: a comparison of change detection techniques. *International Journal of Remote Sensing*, 20(1), 139–152.
- Mertens, B. & Lambin, E. (2000). Land cover change trajectories in southern Cameroon. *Annals of the American Association of Geographers*, 90(3), 467–494.
- Mishra, V. N., Rai, P. K., & Mohan, K. (2014). Prediction of land use changes based on land change modeler (LCM) using remote sensing: A case study of Muzaffarpur (Bihar), India. *Journal of the Geographical Institute Jovan Cvijic, SASA*, 64(1), 111–127.
- Munthali, M., Botai, O., Davis, N., & Abiodun, A. (2019). Multi-temporal Analysis of Land Use and Land Cover Change Detection for Dedza District of Malawi using Geospatial Techniques. *International Journal of Applied Engineering Research*, 14, 1151–1162.
- Odindi, J., Mhangara, P., & Kakembo, V. (2012). Remote sensing land-cover change in Port Elizabeth during South Africa's democratic transition. *South African Journal of Science*, 108(5/6), 1–7.
- Okeke, F. & Karnieli, A. (2006). Methods for fuzzy classification and accuracy assessment of historical aerial photographs for vegetation change analyses. Part I: Algorithm development, 27(1-2), 153–176.
- Paiboonvorachart, C. & Oyana, T.J. (2011). Land-cover changes and potential impacts on soil erosion in the Nan watershed, Thailand. *International Journal of Remote Sensing*, 32, 6587–6609.
- Perumal, K. & Bhaskaran, R. (2010). "Supervised Classification Performance of Multispectral Images," *The Computer Journal*, 2(2), 124–129.
- Petropoulos, G.P., Kalaitzidis, C., & Vadrevu, K.P. (2012). Support vector machines and object-based classification for obtaining land-use/cover cartography from hyperion hyperspectral imagery. *Computer & Geoscience*, 41, 99–107.
- Pflugmacher, D., Cohen, W.B. & Kennedy, R.E. (2012). Using Landsat-derived disturbance history (1972–2010) to predict current forest structure. *Remote Sensing of Environment*, 122, 146–165.
- Pontius, R., Shusas, E., & McEachern, M. (2004). Detecting important land changes while accounting for persistence. *Agricultural Ecosystem Environment*, 101, 251–268.
- Rawat, J.S., Biswas, V. & Kumar, M. (2013). Changes in land use/cover using geospatial techniques: a case study of Ramnagar town area, district Nainital, Uttarkhand, India. *The Egyptian Journal of Remote Sensing and Space Sciences*, 16, 111–117.
- Rwanga, S.S., & Ndambuki, J.M. (2017). Accuracy assessment of land use/land cover classification using remote sensing and GIS. *International Journal of Geosciences*, 8, 611–622.
- Roy, D.P., Wulder, M.A., Loveland, T.R., Woodcock, C.E., Allen, R.G., Anderson, M.C., Helder, D., Irons, J.R., Johnson, D.M., Kennedy, R., Scambos, T., Schaaf, C.B., Schott, J.R., Sheng, Y., Vermote, E.F., Belward, A.S., Bindschadler, R., Cohen, W.B., Gao, F., Hipple, J.D., Hostert, P., Huntington, J., Justice, C.O., Kilic, A., Kovalskyy, V., Lee, Z.P., Lybumber, L., Masek, J.G., McCorkel, J., Shuai, Y., Trezza, R., Vogelmann, J., Wynne, R.H. & Zhu, Z. (2014). Landsat-8: science and product vision for terrestrial global change research. *Remote Sensing Environment*, 145, 154–172.

- Shalaby, A. & Tateishi, R., (2007). Remote sensing and GIS for mapping and monitoring land cover and land-use changes in the Northwestern coastal zone of Egypt. *Applied Geography*, 27, 28–41.
- Shao Y., Fan X., Liu H., Xiao J., Ross S., Brisco B., Brown R. & Staples G. (2001). Rice monitoring and production estimation using multi-temporal RADARSAT. *Remote Sensing Environment*, 76, 310–325.
- Song, C., Woodcock, C.E., Seto, K.C., Lenney, M.P. & Macomber, S.A. (2001). Classification and change detection using Landsat TM data: when and how to correct atmospheric effects? *Remote Sensing Environment*, 75(2), 230–244.
- Story, M., & Congalton, R.G. (1986). Accuracy assessment – A user’s perspective. *Photogrammetric Engineering and Remote Sensing*, 5(23), 397–399.
- Strahler, H. (1980). The use of prior probabilities in Maximum Likelihood Classification of remotely sensed data. *Remote Sensing of Environment*, 10, 135–163.
- Vanonckelen, S., Lhermitte, S. & Van Rompaey, A. (2013). The effect of atmospheric and topographic correction methods on land cover classification accuracy. *International Journal of Applied Earth Observation*, 24, 9–21.
- Wear, D., & Bolstad, P. (1998). Land-use changes in southern Appalachian landscapes: spatial analysis and forecast evaluation. *Ecosystems*, 1, 575–594.
- Wulder, M.A., White, J.C., Loveland, T.R., Woodcock, C.E., Belward, A.S., Cohen, W.B., Fosnight, E.A., Shaw, J., Masek, J.G. & Roy, D.P. (2016). The global Landsat archive: status, consolidation, and direction. *Remote Sensing Environment*, 185, 271–283.
- Yang, X., & Lo, C.P. (2002). Using a time series of satellite imagery to detect land use and cover changes in the Atlanta, Georgia metropolitan area. *International Journal of Remote Sensing*, 23(9), 1775–1798.
- Young, N.E., Anderson, R.S., Chignell, S.M., Vorster, A.G., Lawrence, R. & Evangelista, P.H. (2017). A survival guide to Landsat Pre-processing. *Ecology*, 98(4), 920–932.
- Yuan, F., Sawaya, K. E., Loeffelholz, B. & Bauer, M.E. (2005). Land cover classification and change analysis of the Twin Cities (Minnesota) metropolitan area by multi-temporal Landsat remote sensing. *Remote Sensing of Environment*, 98(2–3), 317–328.
- Zheng, M.G., Cai, Q.G. & Wang Z.J. (2005). Effect of prior probabilities on maximum likelihood classifier, *Proceedings of the 25th IEEE International Geoscience and Remote Sensing Symposium*, 25–29 July, Seoul, Korea: 3753–3756.
- Zhou, G. & Xiong, S. (2012). Comparison of object-oriented and Maximum Likelihood Classification of land use in Karst area. *IEEE International Geoscience and Remote Sensing Symposium*, 6099–6102.